ICAS 2016
30th Congress of the International Council of the Aeronautical Sciences
DCC, Daejeon, Korea ; September 25-30, 2016

NONLINEAR DAMAGE MODELING AND ANALYSIS OF VISCOPLASTIC COMPOSITE MATERIALS

Ill-Kyung Park*, Tae-Uk Kim, and Seung-Ho Kim
***Korea Aerospace Research Institute**

Keywords: *Micromechanical model, Multi-scale approach, Polymeric composite, Rate-dependent damage model, Viscoplasticity*

Abstract

The present study aims at rate-dependent damage modeling for polymeric composite materials with the rate-dependent constitutive model using a multi-scale approach. Phenomenologically, the nonlinear response of a composite under the in-plane shear loading condition is originated from the viscoplasticity of a matrix and the damage behavior of composite materials. In case of dynamic loading conditions, the strain-rate effects the change of the damage behavior of composite materials, as well as the behavior of the matrix. The enhanced micromechanical model which improves the in-plane shear behavior, is used for analyzing the rate-dependent behaviors of the fiber and matrix constituents. The rate-dependent elastic damage model based on orthotropic continuum damage mechanics theory at the macromechanical level is applied to improve the accuracy of the analysis model. Predictions by presented model are shown to agree fairly well with experimental results over a wide range of strain rates.

1 Introduction

Fiber reinforced composite materials with a polymeric matrix have rapidly become the primary materials for aircraft structures, due to the high specific stiffness and strength. Furthermore, increasing demands for eco-friendly transportation systems have encouraged automotive industries to adapt composite materials to improve fuel efficiency.

As crashworthiness is the crucial factor of the design requirements for the structures of the transportation vehicles, it is significant to study design/analysis methodologies of composite structures under severe loading conditions, such as crashes or impacts.

For laminate composite structures composed of orthotropic and heterogeneous fiber reinforced composite materials, the optimal stacking sequence a laminate is typically designed based on dominant static loads under the normal operating conditions. In the events of collisions or crashes, however, transportation vehicles may encounter extreme load conditions with very high strain-rates up to several hundred per second in unexpected directions. Therefore, it is necessary to predict the nonlinear behaviors caused by strain-rates and in-plane shear loading, in order to improve the crashworthiness of composite structures.

The objective of this research is to develop phenomenologically enhanced, effective and accurate analysis method for the nonlinear behaviors of polymeric fiber reinforced unidirectional (UD) composite materials in crash environment. In order to attain the objective, the present study introduces the rate-dependent damage model (RDM) for polymeric composite materials with the state variable inelastic equation for polymers using a multi-scale approach. An enhanced micromechanical model using the modified slicing algorithm is also introduced to improve the accuracy of prediction of in-plane shear stresses. For the verification of the modified slicing algorithm, obtained material properties using proposed model are validated with experimental results [1-3]. The RDM based on an orthotropic continuum damage using a multi-scale approach, predicts the degradation of composite laminates under dynamic loading, it has scalar damage variable which is calculated from the stresses in

each ply. From macromechanical point of view, scalar damage variable is implied into constitutive equations of composite elementary ply which is generated by the enhanced micromechanical approach.

For the verification, developed models are implemented as a UMAT (User Material Subroutine) linked to explicit finite element software, LS-DYNA, and then the computed results are compared to experimentally obtained results for several representative polymeric UD carbon epoxy composite materials.

2 Rate-dependent behavior of polymeric composite laminates

The rate-dependent behavior of polymers is originated from viscoelasticity, viscoplasticity, and variation of failure strength versus strain-rates. Polymers are known to have a rate-dependent deformation response that is nonlinear in range of one or two percent strain. As increasing strain rate, the elastic modulus of polymers typically rises up, while the failure strain of polymers falls off [4]. It is assumed that polymers tend to fail in a brittle manner at high strain rates.

Since carbon fibers is not rate-dependent, the deformation in fiber direction exhibits neither non-linearity nor strain-rate dependence. However, the polymeric composite materials have an equivalent level of rate-dependent properties in matrix dominant directions.

Thiruppukuzhi and Sun [5] proposed the model to present change of failure strength with respect to strain-rate through the experimental study for glass fiber composite materials. The strength parameter kcr can be expressed a function of strain rate, $\dot{\varepsilon}$, as:

$$k_{cr} = k_{cr}^{*}\left(\frac{\dot{\varepsilon}}{\dot{\varepsilon}^{*}}\right)^{\beta} \tag{1}$$

where the * quantities correspond to the reference strain rate and b is material constant determined by the dynamic coupon test. Goldberg [6] and Zheng [7] have applied the rate-dependent strength function to carbon/epoxy composite materials.

3 Rate-dependent polymer model

The isotropic elasto-plastic constitutive equation is applied to the rate-dependent polymer model. Temperature and moisture effects are not considered. The nonlinear strain recovery observed in polymers during unloading is not simulated, and small strain theory is assumed to apply. Phenomena such as creep, relaxation and high cycle fatigue are not accounted for within the equations. The elasto-plastic strain-rate equation can be expressed as:

$$\dot{\varepsilon}_{ij} = \dot{\varepsilon}_{ij}^{e} + \dot{\varepsilon}_{ij}^{I} \tag{2}$$

The total strain rate, $\dot{\varepsilon}_{ij}$, is composed from the elastic component, $\dot{\varepsilon}_{ij}^{e}$, and the inelastic component, $\dot{\varepsilon}_{ij}^{I}$. Since the stresses are only proportioned to the elastic strain, Eq. (2) can be written as:

$$\dot{\varepsilon}_{ij}^{e} = \dot{\varepsilon}_{ij} - \dot{\varepsilon}_{ij}^{I} \tag{3}$$

Eq. (3) can be substituted into the strain components in the constitutive relationship for polymers, then the polymer's constitutive equation can be written as:

$$\dot{\sigma}_{ij} = C_{ijkl}\left(\dot{\varepsilon}_{kl} - \dot{\varepsilon}_{kl}^{I}\right) \qquad i,j,k,l = 1 \ldots 6 \tag{4}$$

The rate-dependent behavior of polymers is implied into the stiffness matrix, C_{ijkl}, as variable elastic modulus by the viscoelastic model for polymers. The inelastic strain rate tensor in Eq. (4) is expressed by the viscoplastic model for polymers.

3.1 Viscoelastic model for polymer

The rate of increasing of an elastic modulus tends to vary in accordance with a range of strain rates [8-10]. This tendency is accounted for by means of definition of the proper viscoelastic model at the lower and upper ranges of strain rates, in this study. The reference strain rate for dividing of the range of strain rates is determined as 200 /s.

The viscoelastic model at the lower range can be expressed as:

$$E = E_0 exp(C_1 \dot{\varepsilon}) \tag{5}$$

Above equation is generated from the dynamic coupon test for the M015 epoxy resin system produced by TB Carbon Company. The dynamic coupon test was conducted using the

constant stroke machine (Instron VHS 8800 High strain rate systems). E is the elastic modulus at the effective strain rate, $\dot{\varepsilon}$, E_0 is the reference elastic modulus, and C_1 is the scaling material constant of the viscoelastic model at the lower range.

To account for the change of the elastic modulus at the upper range of strain rate, we utilize the Johnson-Cool model commonly used to describe the behavior of metals at high strain rates [7, 12]. The viscoelastic model at the upper range for polymers is written as:

$$E = E_0\left(1 + C_2\, ln\frac{\dot{\varepsilon}}{\dot{\varepsilon}_0}\right) \tag{6}$$

C_2 is the scaling material constant of the viscoelastic model at the upper range. The effective strain rate, $\dot{\varepsilon}_0$, is assumed to equal 1/s in this study.

The effective strain rate, $\dot{\varepsilon}$, can be expressed as:

$$\dot{\varepsilon} = \sqrt{\frac{2}{3}[(\dot{\varepsilon}_{11} - \dot{\varepsilon}_m)^2 + (\dot{\varepsilon}_{22} - \dot{\varepsilon}_m)^2 + (\dot{\varepsilon}_{33} - \dot{\varepsilon}_m)^2 + 2\dot{\varepsilon}_{12}^2 + 2\dot{\varepsilon}_{23}^2 + 2\dot{\varepsilon}_{13}^2]} \tag{7}$$

where

$$\dot{\varepsilon}_m = \frac{1}{3}(\dot{\varepsilon}_{11} + \dot{\varepsilon}_{22} + \dot{\varepsilon}_{33})$$

Fig. 1 shows the variation of the elastic modulus with respect to strain rate and the comparison with experimental results and prediction results for the M015 epoxy. The viscoelastic model at the lower range is in good agreement with experimental data up to the reference strain rate, then beyond this value, the viscoelastic model at the upper range is relatively accurate.

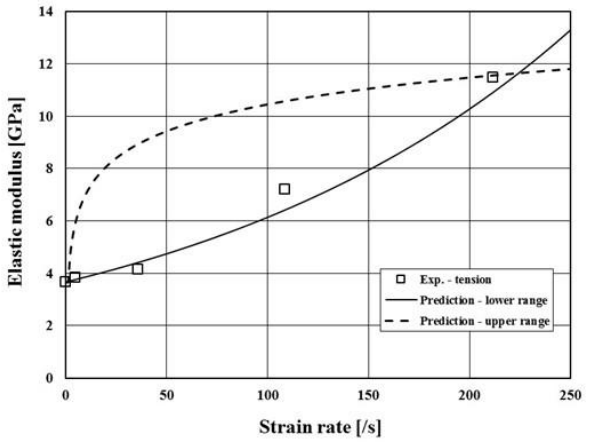

Fig. 1. Variation of Tensile Modulus Versus Strain Rate for M015 Epoxy

3.2 Viscoplastic model for polymer – State variable constitutive equation

To account for the viscoplastic behavior of polymers, the modified Bodner-Partom viscoplastic state variable model, which was originally developed to analyze the viscoplastic deformation of metals above one-half of the melting temperature, is adopted as a viscoplastic model [13]. In the state variable model, a single unified strain variable is defined to represent all inelastic strains. Furthermore, in the state variable approach there is no defined yield stress, Inelastic strains are assumed to be present at all values of stress, the inelastic strains are just assumed to be very small in the "elastic" range of deformation. State variables, which evolve with stress and inelastic strain, are defined to represent the average effects of deformation mechanisms [14]. Since there is no yielding condition, this model is very useful to employ into a numerical analysis method. The viscoplastic constitutive equation for polymers in this study is written as:

$$\dot{\varepsilon}_{ij}^I = 2D_0 exp\left[-\frac{1}{2}\left(\frac{Z}{\sigma_e}\right)^{2n}\right]\left(\frac{S_{ij}}{2\sqrt{J_2}} + \alpha\delta_{ij}\right) \tag{8}$$

The components of the inelastic strain rate tensor are defined as a function of the deviatoric stress components, S_{ij}, the second invariant of the deviatoric stress tensor, J_2, and the isotropic state variable, Z, which represents the resistance to molecular flow. D_0 and n are both material constants, with D_0 representing the maximum inelastic strain rate and n controlling the rate dependence of the material. The effective stress, σ_e, is defined as:

$$\sigma_e = \sqrt{3J_2} + \sqrt{3}\alpha\sigma_{kk} \tag{9}$$

where α is a state variable controlling the level of the hydrostatic stress effects and σ_{kk} is the summation of the normal stress components which equals three times the mean stress.

The rate of evolution of the internal stress state variable, Z, and hydrostatic stress effect state variable, α, are defined follows:

$$\dot{Z} = q(Z_1 - Z)\dot{e}_e^I \tag{10}$$

$$\dot{\alpha} = q(\alpha_1 - \alpha)\dot{e}_e^I \tag{11}$$

where q is a material constant representing the "hardening" rate, and Z_1 and α_1 are material constants representing the maximum value of Z and α, respectively. The initial values of Z and α are defined by the material constants Z_0 and α_0. The effective deviatoric inelastic strain rate, $\dot{e}_e^I$, is defined as:

$$\dot{e}_e^I = \sqrt{\frac{2}{3}\dot{e}_{ij}^I \dot{e}_{ij}^I} \tag{12}$$

where

$$\dot{e}_{ij}^I = \dot{\varepsilon}_{ij}^I - \dot{\varepsilon}_m^I \delta_{ij}$$

$$\dot{\varepsilon}_m^I = \frac{1}{3}(\dot{\varepsilon}_{11}^I + \dot{\varepsilon}_{22}^I + \dot{\varepsilon}_{33}^I)$$

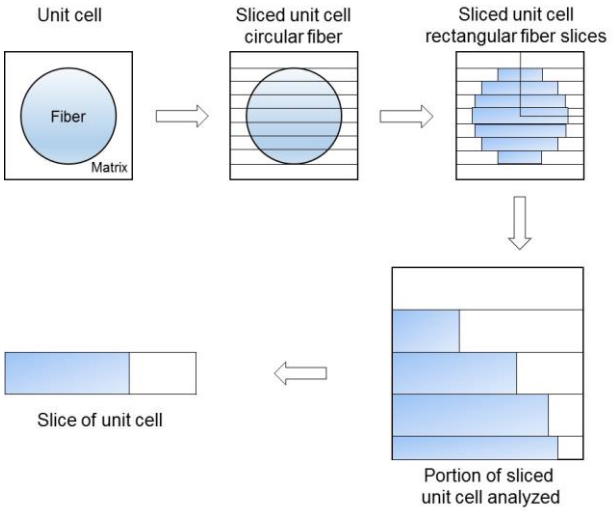

Fig. 2. Schematic Showing Relationship between Unit Cell and Slices for Micromechanics [9,12]

4 Composite micromechanical model

The behavior of polymeric fiber reinforced composite materials is derived from the responses of the individual constituents. Especially, in case of carbon/epoxy composite materials, the strain rate and hydrostatic stress dependent deformations of the polymeric matrix should be considered with the linear and rate-independent behaviors of the carbon fiber simultaneously. To analyze the effectively rate-dependent and nonlinear behaviors of polymeric composite materials, the micromechanical approach has been applied [13]. In the micromechanical model, the unit cell is employed to compute the stress-strain behavior and material properties of a composite lamina.

4.1 Slicing algorithm

Fig. 2 presents the unit cell and slices for the micromechanical approach [9,12]. The unit cell is divided into nine rectangular, horizontal slices and the top and bottom slices in the unit cell are composed of matrix material only. Then each slice is separated into two subslices, one composed of fiber material and the other composed of matrix material. The thickness of horizontal slices are same value except for pure matrix slices. The bottom slice in the analysis cell is one-half as thick as the remaining fiber slices due to symmetry. Each slice has a slice fiber volume fraction, V_f^i, which is defined for the volume average of strains or stresses. The assumptions for the in-plane behavior of the unit cell are made on two levels, the slice level and the unit cell level. At the slice level, along the fiber direction, the strains are assumed to be uniform in each subslice, and the stresses are combined using volume averaging. The in-plane transverse normal stresses and in-plane shear stresses are assumed to be uniform in each subslice, and the strains are combined using volume averaging. The out-of-plane strains are assumed to be uniform in each subslice. The volume average of the out-of-plane stresses in each subslice is assumed to be equal to zero, enforcing a plane stress condition on the slice level. In each slice, the relations between the local strain, ε_{ij}^Fandε_{ij}^M, and the local stresses, σ_{kl}^F and σ_{kl}^M, in the fiber and matrix, respectively, are described as follows:

$$\varepsilon_{ij}^F = S_{ijkl}^F \sigma_{kl}^F \qquad i,j,k.l = 1 \ldots 6 \tag{13}$$

$$\varepsilon_{ij}^M = S_{ijkl}^M \sigma_{kl}^M + \varepsilon_{ij}^{IM} \qquad i,j,k.l = 1 \ldots 6 \tag{14}$$

where S_{ijkl}^M and S_{ijkl}^F, represent the components of the compliance tensors of fiber and matrix materials, respectively. ε_{ij}^{IM} represents the inelastic strains of matrix material. The superscript i and I expresses the slice and the inelastic component, and F and M express fiber and matrix, respectively. The assumptions for stress and strain of each slice can be expressed follows:

$$\varepsilon_{11}^{iF} = \varepsilon_{11}^{iM} = \varepsilon_{11}^i \tag{15}$$

$$\sigma_{11}^{i} = V_f^i \sigma_{11}^{iF} + (1 - V_f^i)\sigma_{11}^{iM} \quad (16)$$

$$\varepsilon_{22}^{i} = V_f^i \varepsilon_{22}^{iF} + (1 - V_f^i)\varepsilon_{22}^{iM} \quad (17)$$

$$\sigma_{22}^{iF} = \sigma_{22}^{iM} = \sigma_{22}^{i} \quad (18)$$

$$\varepsilon_{12}^{i} = V_f^i \varepsilon_{12}^{iF} + (1 - V_f^i)\varepsilon_{12}^{iM} \quad (19)$$

$$\sigma_{12}^{iF} = \sigma_{12}^{iM} = \sigma_{12}^{i} \quad (20)$$

$$\varepsilon_{33}^{iF} = \varepsilon_{33}^{iM} = \varepsilon_{33}^{i} \quad (21)$$

$$\sigma_{33}^{i} = 0 = V_f^i \sigma_{33}^{iF} + (1 - V_f^i)\sigma_{33}^{iM} \quad (22)$$

At the unit cell level, the in-plane strains for each slice are assumed to be constant and equal to the equivalent in-plane strains of the unit cell. The equivalent in-plane stresses of the unit cell are computed using the classical laminate theory (CLT). The strains and stresses in the unit cell are described follows:

$$\begin{Bmatrix} \varepsilon_{11} \\ \varepsilon_{22} \\ \varepsilon_{12} \end{Bmatrix} = \begin{Bmatrix} \varepsilon_{11}^{i} \\ \varepsilon_{22}^{i} \\ \varepsilon_{12}^{i} \end{Bmatrix} \quad i = 1 \ \ldots N_f + 1 \quad (23)$$

$$\begin{Bmatrix} \sigma_{11} \\ \sigma_{22} \\ \sigma_{12} \end{Bmatrix} = \sum_{i=1}^{N_f+1} \begin{Bmatrix} \sigma_{11}^{i} \\ \sigma_{22}^{i} \\ \sigma_{12}^{i} \end{Bmatrix} h_f^i \quad (24)$$

where N_f and h_f^i represent the number of fiber slices in the analysis cell and the ratio of thickness of each slice, respectively. The advantage of the presented micromechanical approach considerably reduced the complexity of the analysis with a high accuracy and efficiency of the computation. Due to this advantage, this model is suitable to apply on the transient structural analysis scheme.

5 Rate-dependent damage model

The RDM presented in this study, starts from this assumption. The composite damage model proposed by Ladeveze [15], which calculates the damage values of each ply using applied stresses and material damage constants, is used as the basic reference damage model in the RDM. To account for the rate-dependence, the viscoplastic model for polymeric matrices using the micromechanical model as previously described, is applied into the RDM as the substitution of the isotropic hardening plastic model in the basic reference damage model.

5.1 Theoretical modeling of the basic reference damage model

The damage process in the matrix is mainly caused by the transverse normal stress, σ_{22}, and in-plane shear stress, σ_{12}. The model assumes that the stress in fiber direction, σ_{11}, does not affect the damage state in the matrix. The basic reference damage model proposed by Ladeveze [15] is theoretically based on the orthotropic continuum damage mechanics, only considers in-plane damages of the elementary ply. In the basic reference damage model, the damaged material strain energy is written as:

$$E_D = \left[\frac{\sigma_{11}^2}{E_{11}^0} - \frac{2\nu_{12}^0}{E_{11}^0}\sigma_{11}\sigma_{22} + \frac{\langle\sigma_{22}\rangle_+^2}{E_{22}^0(1-d_2)} + \frac{\langle\sigma_{22}\rangle_-^2}{E_{22}^0} + \frac{\sigma_{12}^2}{2G_{12}^0(1-d_6)}\right] \quad (30)$$

with $\begin{cases} \langle\sigma\rangle_+ = \sigma & if\ \sigma \geq 0;\ otherwise\ \ \langle\sigma\rangle_+ = 0 \\ \langle\sigma\rangle_- = \sigma & if\ \sigma \leq 0;\ otherwise\ \ \langle\sigma\rangle_- = 0 \end{cases}$

where d_2 and d_6 present the transverse and in-plane scalar damage variables, respectively, that remain constant throughout the ply thickness. The superscript *0* means the initial value, the elastic moduli are kept decreasing by the initiation and evolution of micro-cracks. If the transverse micro-cracks are loaded in compression, they close up and then have no effect on the transverse direction behavior. This explains splitting up the transverse energy into "tension term" and "compression" term in Eq. (30). The associated forces, Y_2^d and Y_6^d, are associated with damage variables, d_2 and d_6, for dissipation, and they are defined follows:

$$Y_2^d = \frac{\langle\sigma_{22}\rangle_+^2}{2E_{22}^0(1-d_2)^2} \quad (32)$$

$$Y_6^d = \frac{{\sigma_{12}}^2}{2G_{12}^0(1-d_6)^2} \quad (33)$$

The damage of a ply is assumed to be governed by the variable Y. The damage variable, Y, is defined as

$$\mathrm{Y} = sup_{\tau \geq t}\sqrt{Y_6^d(\tau) + bY_2^d(\tau)} \quad (34)$$

where b is a material constant which represents the coupling parameter between the effect of the longitudinal and the transverse damaged strain

energies. The damage-development laws are then very simple and are expressed follows:

$$d_2 = \frac{\langle Y - Y_2^0 \rangle_+}{Y_2^c} \tag{35}$$

$$d_6 = \frac{\langle Y - Y_6^0 \rangle_+}{Y_6^c} \tag{36}$$

Therefore, in the basic reference damage model, two directional damages are affected by each other with the material characteristics coupling quantity.

5.2 Development of rate-dependent damage modeling

To validate compatibility between the elastic damage model of the basic reference damage model and the viscoplastic model using the micromechanical approach, the initial RDM which was composed of two models, has been produced. After the analysis results using the initial RDM have compared with experimental results from quasi-static coupon tests, the elastic damage model was modified and applied in the RDM to agree with the experimental data.

Fig. 3 presents the comparison between prediction and experimental results for the $[\pm 67.5°]_s$ angle-ply laminate. In Fig. 3 (a), prediction from the initial RDM with d_2 and d_6, and in Fig. 3 (b), the RDM with only d_6. The prediction is well up to the strain level of 0.3% in Fig. 3 (a). Beyond this point, prediction error starts to occur and increases by about 16% at the maximum strain level of 0.75%. While, in Fig. 3 (b), fairly good agreement between experimental and prediction results till the strain level of 0.5% is observed.

Although prediction error starts to occur beyond this point, there is an only error of about 7%. It can be seen in the comparison between the experimental and prediction results for the [90°] laminate, as shown in Fig. 4. It has been known that the transverse behavior of composite materials is typically linear until the rupture, in case of the initial RDM, however, the nonlinear behavior and the increase of prediction error can be seen after a strain level of 0.2%.

The prediction result from the RDM with only d_6, presents the very good correlation with the experimental result.

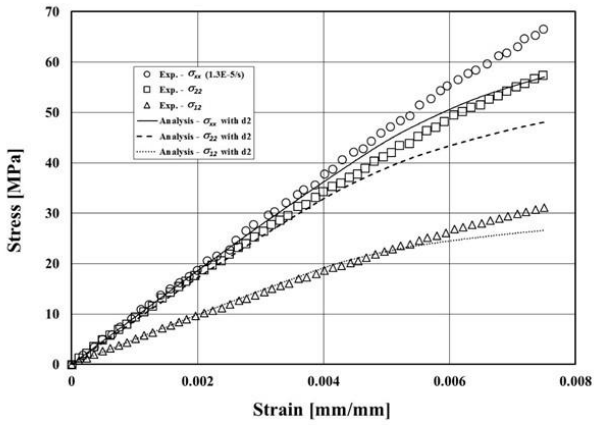

(a)

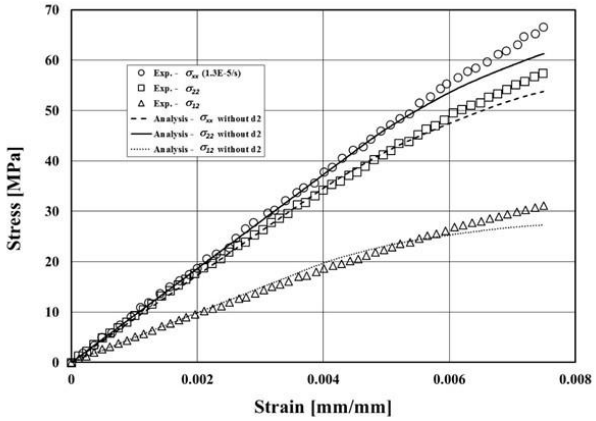

(b)

Fig. 3. Comparison of Experimental and Predicted Stress-Strain Curves for the T700/M015 $[\pm 67.5°]_s$ Laminate: (a) with Transverse Damage Value (d_2); (b) without d_2

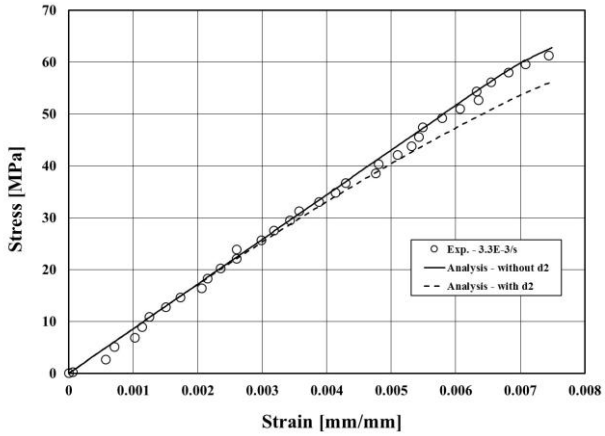

Fig. 4. Comparison of experimental and predicted stress-strain curves for the T700/M015 [90°] with d_2 and without d_2

Through validation of compatibility, these were observed that the initial RDM over-predicts the nonlinear behavior in transverse direction, and the RDM without d_2 has more accurate predictions. It can be assumed that the viscoplastic model presented in this study can

sufficiently simulate not only the transverse nonlinear behavior but also the coupling effect with the in-plane shear behavior. Therefore, it is decided that the in-plane shear damage variable is only considered for the RDM, and the damage variable (Eq. (34)) and damage-development laws (Eq. (35, 36)) in the basic reference damage model can be reduced follows:

$$\mathrm{Y} = sup_{\tau \geq t}\sqrt{Y_6^d(\tau)} \tag{37}$$

$$d_6 = \frac{\langle Y - Y_6^0 \rangle_+}{Y_6^c} \tag{38}$$

To account for change of the damage initiation with respect to strain rate, the in-plane shear initiation damage constant, Y_6^o, is defined follow:

$$Y_6^o = \sqrt{\frac{{\sigma_{12}^{th}}^2}{2G_{12}^0}} \tag{39}$$

The threshold stress of damage, σ_{12}^{th}, is employed to allow to Y_6^o with respect to strain rate. The rate-dependent strength function (Eq. (1)) is applied to obtain σ_{12}^{th} at different strain rates. The threshold stress of damage does not have physical meaning for the strength in the RDM.

To obtain the in-plane shear critical damage constant, Y_6^c, the associated force, Y_6^d, is expressed in terms of σ_{12}^r and d_6 in the following form:

$$Y_6^d = \frac{{\sigma_{12}^r}^2}{2G_{12}^0(1-d_6)^2} \tag{40}$$

substituting Eq. (40) in Eq. (37), and then damage variable, Y, is substituted in Eq. (38), we extract d_6 as a function of σ_{12}^r such as:

$$d_6 = \frac{\sigma_{12}^r}{Y_6^c\sqrt{2G_{12}^0}(1-d_6)} - \frac{Y_6^0}{Y_6^c} \tag{41}$$

At the ruptured shear stress, the quadratic equation for d_6 should have real roots, so we can apply the discriminant on Eq. (46). Finally, Y_6^c is written as:

$$Y_6^c = \frac{\frac{4\sigma_{12}^r}{\sqrt{2G_{12}^0}} - 2Y_6^0 + \sqrt{\left(2Y_6^0 - \frac{4\sigma_{12}^r}{\sqrt{2G_{12}^0}}\right)^2 - 4{Y_6^0}^2}}{2} \tag{42}$$

In Eq. (42), the rupture shear stress, σ_{12}^r, can be also computed by Eq. (1) with respect to strain rate, finally, Y_6^c becomes the rate sensitive constant in the RDM.

5.3 Multi-scale approach for rate dependent damage model

To compute the rate-dependent and nonlinear behaviors of polymeric composite materials based on the response of the individual constituents, a micromechanical approach is employed into the RDM.

The elastic damage value caused by micro-cracks in the matrix or at the matrix/fiber interface is calculated using the ply stresses at the macromechanical level.

6 Model validation

To verify the RDM, experimental results are compared with analysis results for the T700/M015 and IM7/977-2 materials [16]. As part of this study, the T700/M015 is examined for a wide range of strain rates, and this material behaves in somewhat brittle manner. The IM7/977-2 have been frequently used in rate-dependent composite material studies, and it is known that this material has a good toughness property.

To validate the phenomenological maturity and the improvement of the RDM, the analysis results with the elastic damage model ("with DM" in the figure) and without the elastic damage model ("without DM" in the figure), are compared with experimental results.

6.1 Analysis results for T700/M015 material

The RDM is implemented into LS-DYNA as a UMAT, a single shell element model is used for validation of the model. The boundary conditions same as experiments are applied to the model, the constant strain rate is allowed in the model. Dynamic tensile tests for the laminate configuration $[\pm 45°]_s$ of the T700/M015 material were conducted at strain rates of about 2.3E-4/s, about 15~20/s, and about 100~150/s, and these test strain rates

represented a quasi-static, a medium, and a high speed condition, respectively.

Quasi-static tests were carried out using a MTS 810 hydraulic testing machine. Dynamic tests were conducted using an Instron VHS 8800 High strain rate system. Strain gages and an extensor-meter were used to measure the strain data of quasi-static tests, and the digital image correlation method using ARAMIS software was applied to measure the strain data of medium and high strain rate tests.

In case of high strain rate tests in Fig. 5, although the considerable oscillation due to the dynamic effects of the load train of a testing machine is observed, the similar trend of response with other stress-strain curves can be estimated. Fig. 5 presents the comparison between experimental results and prediction results of the analysis model with DM for the $[\pm 45°]_s$ angle-ply at strain rates of 2.3E-4/s, 18.3/s, and 113.6/s. The predicted results fairly agree with the experimental values at quasi-static and medium strain rates.

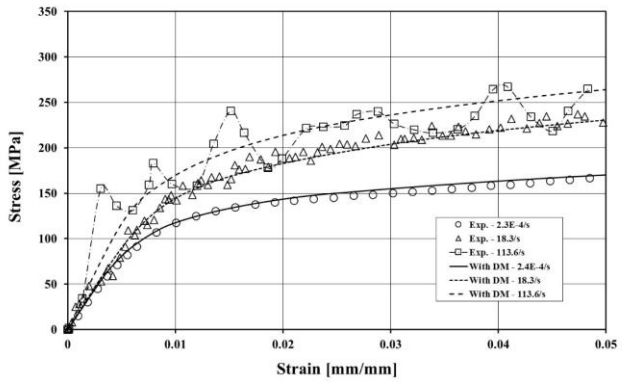

Fig. 5. Comparison of Experimental and Predicted Stress-Strain Curves with Damage Model for T700/M015 $[\pm 45°]_s$ Laminate

The high strain rate result is somewhat under estimation up to the strain level of 1%, beyond this point, prediction correlates well with the tendency of non-linearity.

Specifically, non-linearity and rate dependence of experimental results are captured well qualitatively at the entire range of strain rates.

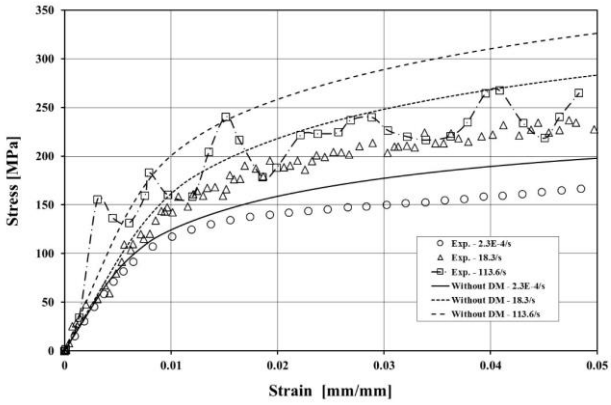

Fig. 6. Comparison of Experimental and Predicted Stress-Strain Curves without Damage Model for T700/M015 $[\pm 45°]_s$ Laminate

Fig. 6 shows the comparison between experimental results and prediction results of the analysis model without DM. Overall, the analysis model overpredicts experimental results significantly beyond a strain level of 0.5%. Moreover, the errors between experimental and prediction results enlarge as increasing strain and strain rate.

6.2 Analysis results for IM7/977-2 material

Gilat et al. [16] have conducted the experimental study for the rate sensitivity of the IM7/977-2 material, and experimental data, was utilized as reference data in several analysis model development researches [9, 11]. Hence, we are willing to apply the IM7/977-2 material on the RDM to compare with other rate-dependent analysis models for polymeric composite materials.

The RDM needs the in-plane initiation damage constant, Y_6^o, which could be obtained by the monotonic tensile coupon test for the $[\pm 45°]_s$ laminate as previously described. However, it is impossible to execute the monotonic tensile test with the same composite material, in this study, the value of Y_6^o is estimated through the analysis of the initiation of non-linearity for the $[\pm 45°]_s$ laminate tensile test data [16] with a assistance of FE analysis. The viscoelastic model written in Eq. (6) is only

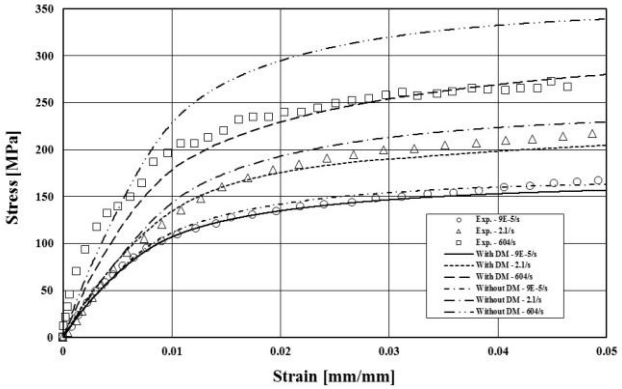

Fig. 7. Comparison of Experimental [9] and Predicted Stress-Strain Curves with and without Damage Model for IM7/977-2 $[\pm 45°]_s$ Laminate

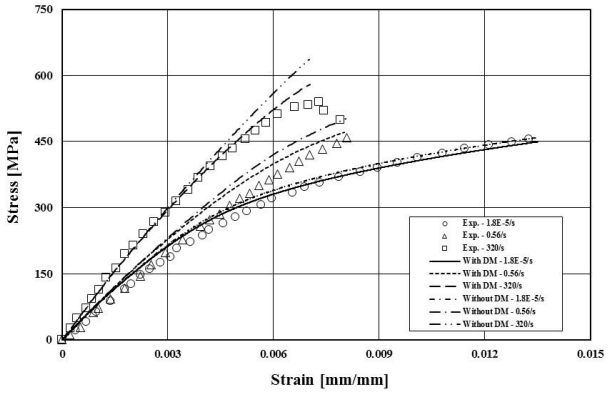

Fig. 8. Comparison of Experimental [9] and Predicted Stress-Strain Curves with and without Damage Model for IM7/977-2 [10°] Laminate

applied to the IM7/977-2 material at all of strain rates, because the scaling material constant, C_2, is just available.

Fig. 7 shows the comparison between experimental results and prediction results of the analysis model with DM and without DM. Throughout all of strain rates, the analysis model with DM is more accurate than without DM. In case of with DM, the prediction results fairly agree with the experimental values for the quasi-static and medium strain rates up to the strain level of 2%. Beyond this point, the quasi-static result keeps a good correlation, while the medium strain rate is somewhat under prediction of the stress as increasing strain. At high strain rate, prediction result is somewhat under estimation up to the strain level of 3%, beyond this point, prediction correlates well with the experimental data.

In case of without DM, the errors of prediction results are grown up as increasing strain and strain rate, which results are same as the T700/M015 material.

Figs. 6 and 7 depict the verification results of off-axis loading conditions, and show the [10°] and the [45°], respectively. Two comparison results show that the analysis model with DM is more accurate than without DM. Though it is similar to previous comparison cases, predictions from two analysis models are similar to each other. Relatively little discrepancies between two models are most likely due to a small range of strain.

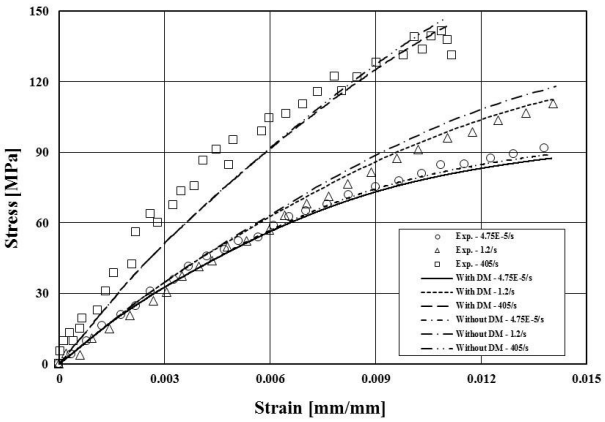

Fig. 9. Comparison of Experimental [9] and Predicted Stress-Strain Curves with and without Damage Model for IM7/977-2 [45°] Laminate

In Fig. 8, at high strain rates, the analysis result fairly agrees with the experimental data, but the over estimations are observed at quasi-static and medium strain rates. Beyond a strain level of 0.8%, however, the quasi-static result is well correlation with the experimental data. In Fig. 9, at high strain rates, the analysis model is somewhat under prediction of stress up to 0.9%, while the prediction results at quasi-static and medium strain rates are in good agreement with experimental results.

6 Conclusions

In this work, the phenomenological inquiry for polymeric UD carbon composite materials is carried out with the sources of nonlinear deformations such as anisotropic behavior, rate-dependent characteristics, and the initiation and evolution of micro-cracks.

The viscoelastic and viscoplastic constitutive equations are employed to simulate the rate-dependence of polymers. The micromechanical approach is employed to consider the different response of constituents simultaneously. The enhanced micromechanical model using the modified slicing algorithm is proposed to improve the prediction of in-plane shear behavior, and the verification is carried out through comparisons with several coupon test results.

To account for the damage from the micro-cracks in the matrix and the matrix/fiber interface, the rate-dependent elastic composite damage model is introduced and modified as a simple form through validation to ensure compatibility with the viscoplastic model using a micromechanical approach. Finally, the RDM using a multi-scale approach is developed, and then the implementation of LS-DYNA as a UMAT is carried out.

Through validation of the RDM using a multi-scale approach with experimental results of the T700/M015 and IM7/977-2 materials, it is confirmed that the RDM using a multi-scale approach precisely captures the non-linearity and rate dependence of polymeric composite materials with wide range of toughness under in-plane shear dynamic loading, qualitatively and quantitatively.

References

[1] W. Y. You, J. H. Lim, D. W. Sohn, S. W. Kim, S. H. Kim, Prediction of the equivalent elastic properties of fiber reinforced composite materials and structural analysis of composite satellite panel, Aerospace Eng. Technol. Vol. 12, No 2, pp 48-56, 2013.

[2] C. T. Sun, R. S. Vaidya, Prediction of composite material properties from a representative volume element, Compos. Sci. Technol. Vol. 56, pp 171-179, 1996.

[3] J. Y. Jeong, S. K. Ha, Analysis of micromechanical behavior of fiber-reinforced composites, The Transactions of the Korean Society of Mech. Eng. A, Vol. 28, No 10, pp 1435-1450, 2004.

[4] A. Gilat, R. K. Goldberg, Experimental study of strain rate dependent behavior of carbon/epoxy composite, Compos. Sci. Technol. Vol 62, pp 1469-1476, 2002.

[5] S. V. Thiruppukuzhi, C. T. Sun, Models for the strain-rate-dependent behavior of polymer composites, Compos. Sci. Technol. Vol 61, pp 1-21, 2001.

[6] R. K. Goldberg, Strain rate dependent deformation and strength modeling of a polymer matrix composite utilizing a micromechanics approach, NASA/TM-1999-209768, Washington, DC, NASA, 1999.

[7] X. Zheng, Nonlinear strain rate dependent composite model for explicit finite element analysis, PhD Dissertation, University of Akron, Akron, Ohio, 2006.

[8] A. Gilat, R. K. Goldberg, Strain rate sensitivity of epoxy resin in tensile and shear loading, NASA/TM-2005-213595, Washington, DC, NASA, 2005.

[9] R. K. Goldberg, Computational simulation of the high strain rate tensile response of polymer matrix composites, NASA/TM-2002-211489, Washington, DC, NASA, 2002.

[10] A. D. Mulliken, Low to high strain rate deformation of amorphous polymers: Experiments and modeling, M.Sc. Dissertation, Massachusetts institute of technol., Cambridge, Massachusetts, 2004.

[11] X. Zheng, Nonlinear strain rate dependent composite model for explicit finite element analysis, PhD Dissertation, University of Akron, Akron, Ohio, 2006

[12] C. F. Yen, Ballistic impact modeling of composite materials, Proceeding of the 7th int. LS-DYNA users conference, 2002.

[13] R. K. Goldberg, D. R. Gary, A. Gilat, Implementation of an associative flow rule including hydrostatic stress effects into the high strain rate deformation analysis of polymer matrix composites, NASA/TM-2003-212382, Washington, DC, NASA, 2003.

[14] X. Zheng, R. K. Goldberg, W. K. Binienda, G. D. Roberts, LS-DYNA implementation of polymer matrix composite model under high strain rate impact, NASA/TM-2003-102633, Washington, DC, NASA, 2003.

[15] P. Ladeveze, E. Le Dantec, Damage modelling of the elementary ply for laminated composites, Compos. Sci. Technol. Vol 43, pp 257-267, 1992.

[16] A. Gilat, R. K. Goldberg, G. D. Roberts, Experimental study of strain-rate-dependent behavior of carbon/epoxy composite, Compos. Sci. Technol. Vol 62, pp 1469-1476, 2002.

Copyright Statement